BRAIN
ORIGINAL ARTICLE

Normative intracranial EEG maps epileptogenic tissues in focal epilepsy

John M. Bernabei,[1,2,†] Nishant Sinha,[1,2,3,†] T. Campbell Arnold,[1,2] Erin Conrad,[2,3] Ian Ong,[1,2] Akash R. Pattnaik,[1,2] Joel M. Stein,[4] Russell T. Shinohara,[5,6,7] Timothy H. Lucas,[8] Dani S. Bassett,[1,3,9,10,11,12] Kathryn A. Davis[2,3] and Brian Litt[1,2,3,8]

[†]These authors contributed equally to this work.

Planning surgery for patients with medically refractory epilepsy often requires recording seizures using intracranial EEG. Quantitative measures derived from interictal intracranial EEG yield potentially appealing biomarkers to guide these surgical procedures; however, their utility is limited by the sparsity of electrode implantation as well as the normal confounds of spatiotemporally varying neural activity and connectivity. We propose that comparing intracranial EEG recordings to a normative atlas of intracranial EEG activity and connectivity can reliably map abnormal regions, identify targets for invasive treatment and increase our understanding of human epilepsy.

Merging data from the Penn Epilepsy Center and a public database from the Montreal Neurological Institute, we aggregated interictal intracranial EEG retrospectively across 166 subjects comprising >5000 channels. For each channel, we calculated the normalized spectral power and coherence in each canonical frequency band. We constructed an intracranial EEG atlas by mapping the distribution of each feature across the brain and tested the atlas against data from novel patients by generating a z-score for each channel. We demonstrate that for seizure onset zones within the mesial temporal lobe, measures of connectivity abnormality provide greater distinguishing value than univariate measures of abnormal neural activity. We also find that patients with a longer diagnosis of epilepsy have greater abnormalities in connectivity. By integrating measures of both single-channel activity and inter-regional functional connectivity, we find a better accuracy in predicting the seizure onset zones versus normal brain (area under the curve = 0.77) compared with either group of features alone.

We propose that aggregating normative intracranial EEG data across epilepsy centres into a normative atlas provides a rigorous, quantitative method to map epileptic networks and guide invasive therapy. We publicly share our data, infrastructure and methods, and propose an international framework for leveraging big data in surgical planning for refractory epilepsy.

1 Department of Bioengineering, University of Pennsylvania, Philadelphia, PA 19104, USA
2 Center for Neuroengineering and Therapeutics, University of Pennsylvania, Philadelphia PA 19104, USA
3 Department of Neurology, Penn Epilepsy Center, Hospital of the University of Pennsylvania, Philadelphia, PA 19104 USA
4 Department of Radiology, Hospital of the University of Pennsylvania, Philadelphia, PA 19104, USA
5 Department of Biostatistics, Epidemiology, and Informatics, University of Pennsylvania, Philadelphia, PA 19104, USA
6 Statistics in Imaging and Visualization Center, University of Pennsylvania, Philadelphia, PA 19104, USA
7 Center for Clinical Epidemiology and Biostatistics, University of Pennsylvania, Philadelphia, PA 19104, USA
8 Department of Neurosurgery, Hospital of the University of Pennsylvania, Philadelphia, PA 19104, USA
9 Department of Electrical & Systems Engineering, University of Pennsylvania, Philadelphia, PA 19104, USA
10 Department of Physics & Astronomy, University of Pennsylvania, Philadelphia, PA 19104, USA
11 Department of Psychiatry, University of Pennsylvania, Philadelphia, PA 19104, USA
12 The Santa Fe Institute, Santa Fe, NM 87501, USA

Correspondence to: John Bernabei
Hayden Hall room 301
University of Pennsylvania

Received August 14, 2021. Revised November 14, 2021. Accepted November 26, 2021. Advance access publication May 31, 2022

240 South 33rd Street
Philadelphia, PA 19104, USA
E-mail: John.Bernabei@pennmedicine.upenn.edu

Correspondence may also be addressed to: Nishant Sinha
E-mail: nishant.sinha89@gmail.com

Keywords: epilepsy; intracranial EEG; functional connectivity; brain network model; epilepsy surgery

Abbreviations: HFO = high-frequency oscillation; HUP = Hospital of the University of Pennsylvania; iEEG = intracranial EEG

Introduction

For over 20 million patients with drug-resistant focal epilepsy,[1] surgery offers the best chance at seizure freedom. An effective surgical plan relies on accurately delineating brain regions that can generate seizures, known as the epileptogenic zone.[2] In many patients, clinicians cannot localize the epileptogenic zone through purely noninvasive measures, such as scalp EEG, ictal semiology, neuropsychological testing and neuroimaging, and instead rely on recording seizures directly using intracranial EEG (iEEG). These implanted electrodes record electrographic activity across large cortical and subcortical areas at a high temporal resolution. However, the current paradigm of subjective and qualitative interpretation may lead to an inappropriate selection of surgical targets, perhaps partially explaining the fact that 40% of patients fail to achieve seizure freedom.[3,4] Furthermore, patients with iEEG must remain hospitalized for weeks in specialized monitoring units awaiting spontaneous seizures, which is associated with the high cost and low accessibility of epilepsy surgery.[5] There is an urgent need to improve the approach to epilepsy surgery by developing reliable quantitative measures to identify epileptogenic tissues before surgery and predict the likelihood of seizure recurrence after different device and surgical interventions.

The two prevailing hypotheses that guide epilepsy surgery are that (i) the epileptogenic zone is a discrete circumscribed region that must be removed; or (ii) the epileptogenic zone is part of a distributed network that cannot be fully removed.[6] Traditional iEEG practice reflects the first hypothesis and relies upon capturing qualitatively abnormal iEEG activity, such as focal spikes and patterns of well-localized seizure onset[7,8] at the level of individual channels.[9,10] Beyond these paroxysmal events, epileptogenic regions may also cause focal differences in baseline rhythmic activity, such as slowing, between seizures.[11] Studies that apply graph theory to iEEG provide increasing evidence that epilepsy arises from disordered brain networks, but there are nuances that have prevented their effective clinical translation.[12–20] While many approaches successfully identify the epileptogenic zone and predict surgical outcome, these studies suffer from sampling bias which can vary by graph metric and by electrode type.[21,22] Beyond sampling bias, quantitative methods of mapping epileptic networks are confounded by normal variation in the spatial patterns of neural activity[23] and connectivity.[24] Approaching iEEG data as containing important information that is both spatially localized (consistent with the first hypothesis) and spatially distributed (consistent with the second hypothesis) could benefit epilepsy surgery. To our knowledge, only one study combined the iEEG measurements at the electrode-level and the network-level to quantify seizure onset.[25] For reliably mapping epileptogenic tissues, we anticipate that it will be crucial to assess electrode-level activity and network-level connectivity measurements in a common framework while controlling for the baseline deviations expected across the brain.

Normative modelling offers a promising approach to robustly map abnormal brain areas in a patient.[26–28] This approach uses data from healthy subjects to estimate a normal baseline range of a given metric, and then quantifies abnormalities by the amount that a metric's value deviates from the normal range. Indeed, the normative modelling framework is flexible enough to probe abnormalities in nodal activity and in inter-nodal connectivity. While normative modelling that leverages widely available non-invasive imaging data of healthy subjects is routine,[29] clinicians very rarely implant iEEG electrodes in patients without epilepsy. However, recent work has shown that aggregating a high number of non-epileptogenic iEEG channels across a large cohort can permit the estimation of normative iEEG neural activity[23] and functional connectivity.[24] We therefore expect that comparing patients' interictal quantitative iEEG features against the normative population will allow us to identify regions that can generate spikes and seizures.

Here, we expand a previously published normative iEEG atlas[23] by harmonizing it with additional data from good outcome epilepsy patients. Further, we estimate a normal range of fluctuations in band-power and functional connectivity strength. In each patient, we quantify abnormalities in brain regions as deviations from the normal range, both in regional iEEG activity and regional connectivity profiles measurements. We hypothesize the following: (i) these measurements from epileptogenic tissue are more abnormal than the same measurements from non-epileptogenic tissue; (ii) that abnormalities in band-power and connectivity measurements provide complimentary information; and (iii) these abnormalities correlate with a range of clinically important phenomena. We also open our collaborative framework and publicly release our iEEG data and atlas so that others can build upon our data and methods. Overall, we aim to establish a framework for collaboratively aggregating data, knowledge and experience across centres in a rigorous way, with the goal of globally improving invasive treatment for epilepsy.

Patients and methods

We retrospectively analysed data from 166 patients with drug resistant epilepsy. Sixty of these subjects underwent iEEG implantation as part of presurgical evaluation at the Hospital of the University of Pennsylvania (HUP). As no single centre has a high enough volume to support the construction of a comprehensive iEEG atlas, we leveraged a high-quality, publicly available iEEG dataset of 106 subjects at the Montreal Neurological Institute (MNI) and two other centres, specifically 1772 channels of their data that were judged as clinically normal and released as the MNI Open iEEG Atlas (https://mni-open-ieegatlas.research.mcgill.ca).[23] Across the multicentre cohort, each patient underwent implantation with

Table 1 Summary of demographics of patient cohort

	Latest surgical outcome		P-value
	Engel 1	Engel 2+	
Number of patients	38	22	
Sex			0.46[a]
Female	17	12	
Male	21	10	
Laterality			0.50[a]
Right	19	9	
Left	19	13	
Pre-surgical MRI			0.05[a]
Lesional	22	7	
Non-lesional	16	15	
Age onset	14.9 ± 11.7	17.5 ± 14.5	0.63[b]
Age surgery	38.8 ± 10.8	35.2 ± 11.8	0.69[b]
Target			0.39[a]
Temporal	28	14	
Frontal	7	6	
Parietal	2	0	
Insular	1	2	
Implant type			**0.008**[a]
Electrocortiography	20	4	
Stereo-EEG	18	18	
Surgery type			**0.01**[a]
Resection	25	7	
Ablation	13	15	
Node count			
Total in grey matter	82.1 ± 25.1	91.8 ± 30.5	0.16[b]
Removed	12.3 ± 10.7	8.5 ± 6.2	0.12[b]
Initially Engel 1 before relapse	N/A	8	

Patients were grouped by initial surgical outcome. Left column shows patients that achieved Engel 1 outcome at 6 months. Right column shows patients that had poor surgical outcome at 6 months.
[a]Rank-sum test.
[b]Pearson Chi-square test.

subdural grid and strip electrodes (electrocortiography), only depth electrodes (stereo-EEG) or a mixture of both. At HUP, all subjects underwent either resection or laser ablation after electrode explant. We also determined surgical outcome on the Engel scale at a minimum of 6 months after surgery, and at the 12-month and 24-month post-operative interval for the majority of patients. Thirty-eight HUP patients had a good surgical outcome (Engel 1) at their most recent follow-up, whereas the remaining 22 subjects had Engel 2+ outcome. All subjects consented to data collection and sharing, and we performed all research through protocols approved by the Institutional Review Board of the University of Pennsylvania. The overall characteristics of the HUP cohort are described in Table 1, and we include patient-specific data in Supplementary Table 1.

Data selection

We selected 60 s of data in two 30-s clips for each subject that met the following criteria in order of priority: (i) free of artefact; (ii) at least 2 h before the beginning of a seizure and at least 2 h after a subclinical seizure, 6 h after a focal seizure or 12 h after a generalized seizure; (iii) free of spikes if possible; and (iv) not within the first 72 h of recording to minimize immediate implant and anaesthesia effects. All selected clips met conditions (i) and (ii), and the majority of clips met conditions (iii) and (iv). We used clips that captured awake brain activity, determined both by the selection of daytime epochs and the use of a custom non-REM sleep detector developed using MNI data and validated on HUP data (Supplementary material). We first montaged the HUP data into a bipolar configuration to match that of the MNI Open iEEG Atlas. We used a first-order Butterworth filter with a passband of 0.5 to 80 Hz to remove high-frequency oscillations (HFOs), and we also applied a 60 Hz IIR notch filter to remove line noise. To match the MNI atlas, we down-sampled the data to 200 Hz from its original 512 or 1024 Hz sampling rate. We excluded any channels contaminated by clear artifact as well as bipolar pairs in which both contacts were in white matter, or either contact was located outside of the brain.

As our study requires a distinction between clinically normal and abnormal regions, we also used a validated algorithm to detect and quantify interictal spikes[9] (Supplementary material). We considered a region that generates at least one spike per hour to be part of the irritative zone.[2] We also recorded clinically-determined seizure onset zones as marked by fellowship-trained neurologists in the official report from the patients stay in the epilepsy monitoring unit. We included all seizure onset zones including subclinical events and did not distinguish between a patient's primary seizure type and secondary semiologies.

Each HUP patient underwent a standard epilepsy imaging protocol including pre- and post-implant 3D T_1-weighted MRI and post-implant CT. Using Advanced normalization tools,[30] the post-implant imaging was registered to the pre-implant MRI, which was separately registered to MNI space for use with neuroimaging atlases. Electrode contact coordinates were derived from the post-implant CT using custom software and localizations confirmed by visualization in ITK-SNAP.[31] We then registered the pre-implant MRI into MNI space for use with neuroimaging atlases. Finally, we used a semi-automated algorithm previously described and validated[20] to perform resection and ablation zone segmentations which determine the electrode contacts targeted by surgery.

Construction of the MNI-HUP intracranial EEG atlas

To ensure that data from our centre could be compared and combined with the 1772 channels of normative MNI data (Fig. 1A), we implemented a rigorous data selection process that closely followed the gold-standard methods of Frauscher *et al.*[23] Similar to the MNI dataset, we defined an abnormal channel as one that is within the seizure onset zone, irritative zone, or was within the resection zone. In traditional epilepsy surgery, normal tissue may be resected due to surgical considerations. In our cohort, only 56 out of 2899 abnormal channels were resected but not determined to be in the irritative or epileptogenic zones. We grouped these 56 channels with the rest of the abnormal channels to ensure we did not use any of these channels in our strict definition of channels which represent normative activity. This process yielded 532 clinically normal HUP channels (Fig. 1B) and 2899 clinically abnormal channels. Using MNI coordinates, we mapped each channel onto the automated anatomical labelling atlas (Fig. 1C). However, we eliminated regions that are not typically targeted by iEEG, including the cerebellum and basal ganglia, and further aggregated neighbouring gyri in regions with low sampling to increase the samples in each region. This process reduced the number of regions of our atlas to 20 in each hemisphere and permitted a higher coverage of inter-regional edges from which we could estimate normative connectivity when compared with automated anatomical labelling (Supplementary Figs 1 and 2). After ensuring similar bandpower in the HUP and MNI datasets (Fig. 1D and Supplementary Fig. 3), we finally combined normative HUP and MNI data into a composite iEEG atlas consisting of 2304 channels across the brain (Fig. 1E).

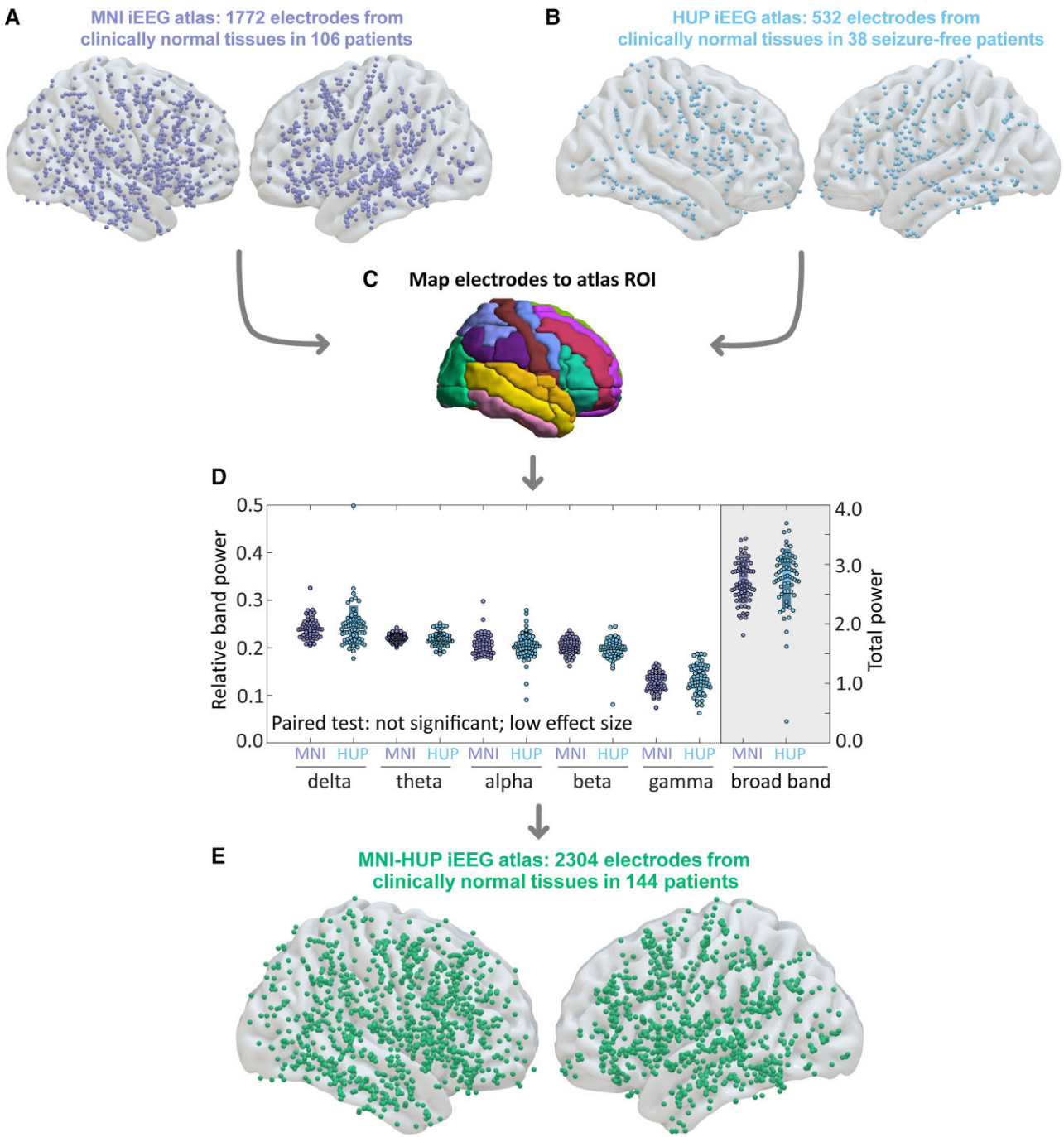

Figure 1 Construction of our normative iEEG atlas. (**A**) We aggregated 1772 normal channels across 106 patients from the MNI open iEEG atlas with (**B**) 532 clinically normal channels from 38 HUP patients. (**C**) We localized each channel to a region in a predefined atlas. (**D**) We did not observe significant differences in relative band power between HUP and MNI atlases. (**E**) Combining HUP and MNI data yielded a total composite, normative iEEG atlas of 2304 channels across 144 patients. ROI = region of interest.

Detecting intracranial EEG electrographic abnormalities

In every patient, for each 'test' iEEG electrode contact, we identified a set of electrode contacts implanted in the same brain area in the normative HUP-MNI iEEG atlas (Fig. 2A and B). In both 'test' and normative channels, we calculated the power spectral density from 0.5 to 80 Hz in 0.5 Hz steps (Fig. 2C) using Welch's method[32] with a 2-s Hamming window and a 1-s overlap. We normalized the spectral density to have a sum of 1 as surface and depth electrodes may have different impedances and therefore signal amplitude, but preserved frequency content.[23] Thus, our method allows us to determine whether the distribution of power across frequency bands differs from the normative distribution, but not whether absolute power is abnormally low or high. We calculated normalized spectral content in the following frequency bands: delta (0.5–4 Hz), theta (4–8 Hz), alpha (8–12 Hz), beta (12–30 Hz) and gamma (30–80 Hz),

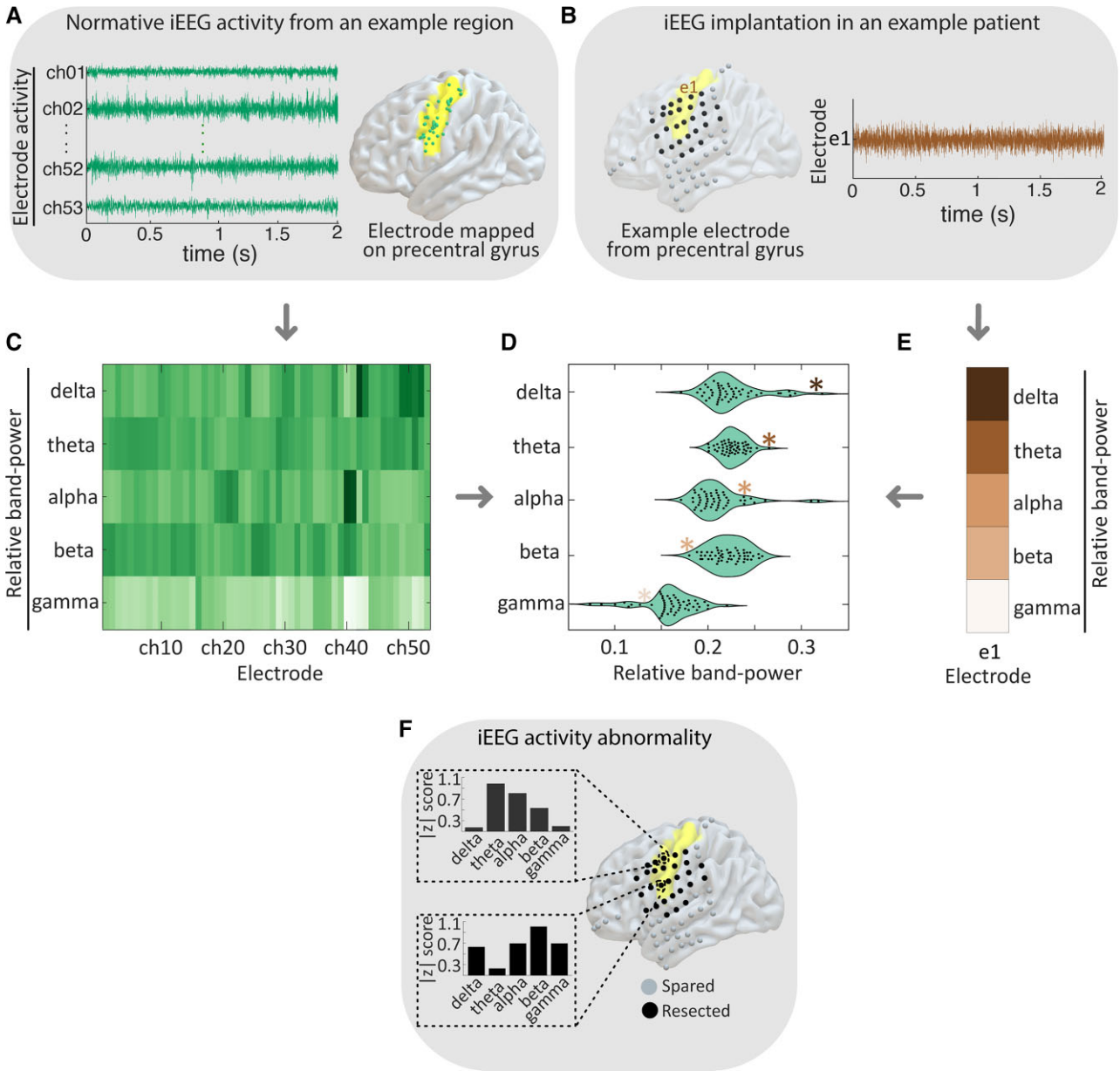

Figure 2 Mapping abnormalities of iEEG spectral activity. (**A**) We aggregate all normative channels within a given region. (**B**) In an example test patient, we select each channel. (**C**) We calculate the power in each frequency band for each normative electrode and estimate the normal distribution across channels. (**D**) Comparison between the calculated relative band-power of the test channel shown in **E** with normative distribution in **C**. (**F**) This process yields a |z| score of spectral activity for each frequency band at each electrode contact in the test patient.

taking the median value within each band. We compared the 'test' channel's spectral features to those of the normative HUP-MNI iEEG atlas in the same region (Fig. 2D and E), which yielded z-scores of spectral density for each channel in the test patient (Fig. 2F). We completed this process for each channel in each patient so that all channels in our study received a z-score of spectral density in each frequency band. As we were concerned primarily with the presence and not the directionality of any abnormality, we took the absolute value of each z-score. Thus, each of the 2304 normative and 2899 abnormal channels across patients received a |z| score of neural activity abnormality in each frequency band.

Mapping iEEG network abnormalities

We also developed methods for assessing the abnormality of functional connectivity using the normative iEEG atlas. For each patient, we divided the interictal epoch into 1-s intervals and computed the median coherence between each pair of channels over time to obtain a single subject-specific adjacency matrix for each of the five aforementioned frequency bands. Each of the edges in each patient's adjacency matrix were then standardized against the distribution of normative atlas edges between the same pair of brain regions (Fig. 3A–F). These steps transformed the coherence value for each pair of channels in a patient to a measure of connectivity

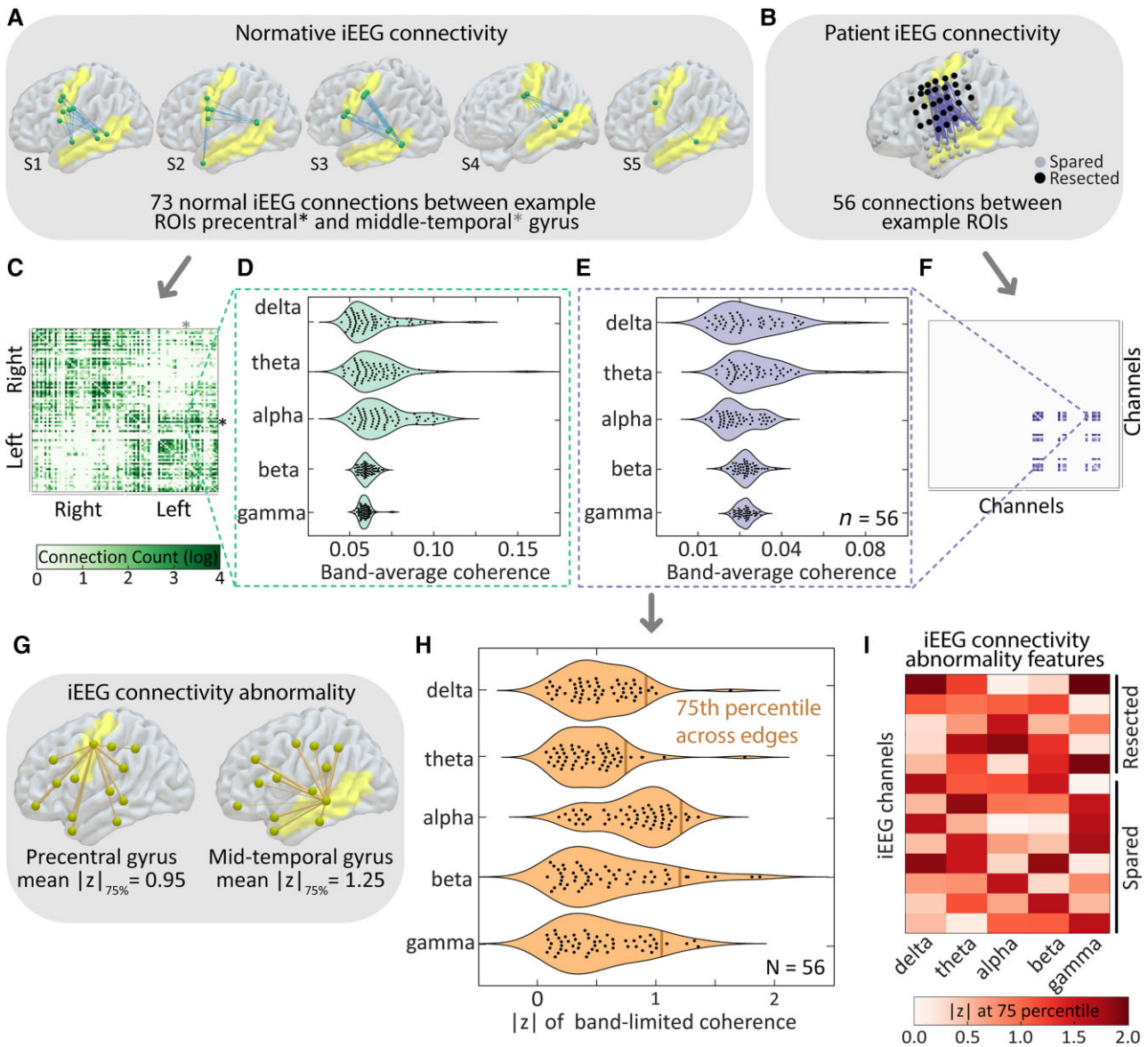

Figure 3 Mapping abnormalities of iEEG functional connectivity. (**A**) We aggregate normative connectivity between pairs of regions and (**B**) compare it to connections between the same pair of regions in a test subject. (**C**) Across all inter-regional pairs we calculate connectivity in each frequency band (**D**). (**E**) We also calculate connectivity in the test patient in each frequency band comprising an adjacency matrix in the test patient (**F**). In order to calculate abnormality scores for each node (**G**), we calculate the 75th percentile |z| across all edges for each node (**H**), yielding a single connectivity abnormality feature for each channel (**I**).

abnormality, where the value of each edge represents the distance between observed value of coherence and the expected, normative connectivity between the pair of sampled regions. As before, we calculated the absolute value of z-scores to detect the presence rather than the direction of abnormalities. Since each channel has a large number of edges representing its connections to other channels in that patient, we required a method to assign it a single value representing its overall connectivity abnormality within each frequency band. Thus, we assigned the 75th percentile across all edge |z| scores for each channel (Fig. 3G and H). We chose the 75th percentile as it captured a high level of abnormality but was not as sensitive to outliers as the maximum edge weight value for each node. This process yielded a single connectivity abnormality feature for each channel (Fig. 3I).

Statistical methods

When calculating abnormality scores for electrographic and network abnormalities, we pooled all normative channels in a given region across patients to estimate the expected feature mean and variance rather than first averaging within-patient. We did not observe significant differences between channel-wise and patient-wise pooling in a limited analysis (Supplementary Fig. 4). To predict the epileptogenic nature of each channel, we developed a random forest algorithm to distinguish normative channels from those that were marked as located within the seizure onset zone and subsequently resected. In our random forest classifier, the training labels and ground truth of the 'epileptogenic' class were seizure onset nodes within the resection zone, whereas the ground

truth for the 'normal tissue' class were non-resected nodes that were not in the seizure onset or irritative zones. Using 10-fold cross-validation at the patient level, we trained the algorithm and then applied it to all channels across each subject, including those which were neither clinically normal nor within the resected seizure onset zone. We quantified overall classifier performance using the area under the receiver operating characteristic curve (AUC) and compared the performance between the full feature set and models trained using only univariate or only bivariate features. From the random forest output, we selected the probability that each channel was in the resected seizure onset zone as a proxy of epileptogenicity. The area under the precision-recall curve (AUPRC) is a binary classification performance metric that is better for rare events and independent of model specificity.[33] We chose this metric for quantifying classifier performance on a per-patient level because within each patient, especially those which underwent focal laser ablation, the number of channels targeted by surgery is small compared with the total number of channels. Thus, a higher level of AUPRC meant that the predicted epileptogenicity better aligned with the resection or ablation zone.

Data availability

In the interest of helping network techniques such as ours reach clinical practice, we share all code and data from this study. All pre-implant, post-implant, and post-resection or ablation imaging as well as full intracranial EEG records are available at ieeg.org[34] using the patient IDs available in Supplementary Table 2. All code as well as .mat files containing the processed atlas adjacency matrices, and information about clinical metadata is available at GitHub.com/jbernabei/iEEG_atlas. The HUP Open iEEG Atlas is publicly available at https://discover.pennsieve.io/datasets/179. A description of each of the data fields contained within the file is available in Supplementary Table 2.

Results

Mapping univariate abnormalities in neural activity

We first sought to determine whether abnormalities in interictal spectral content robustly identify regions that generate spikes and seizures. We compared the median normalized spectral density in each frequency band and each brain region (aggregating nodes from the same region in each hemisphere) between datasets using the rank-sum test and adjusted the significance level to $\alpha = 0.0005$ to correct for 100 comparisons (20 regions × 5 frequencies). We show the results for the eight regions with the largest number of resected electrodes in the atlas (Fig. 4; see Supplementary Fig. 5 for the remaining regions). We found that in many regions, the irritative and seizure onset zones were distinguishable from healthy, uninvolved brain represented by the normative atlas in at least one frequency band. In many cases, particularly in the fusiform gyrus, inferior temporal gyrus, and medial frontal gyrus, the spectral density curve had a relatively steeper fall-off than uninvolved brain, resulting in higher amounts of low-frequency activity and lower amounts of high-frequency content. However, in other clinically relevant regions making up the mesial temporal lobe, including the hippocampus, amygdala and parahippocampal gyrus, we observed no discernable difference in spectral content between normal and epileptogenic tissue. In comparison with normalized spectral density features, we found that within-patient absolute bandpower did not reliably discriminate between epileptogenic and normal tissues (Supplementary Fig. 6). These findings imply that clinical abnormalities often, but not always, result in region-specific aberrations in spectral content. Thus, we also mapped abnormalities in interictal connectivity to better distinguish clinically normal and abnormal channels.

Mapping abnormalities using bivariate features

Based on the observation that the univariate feature of spectral density did not effectively distinguish mesial temporal lobe channels that generated spikes and seizures from those that did not,

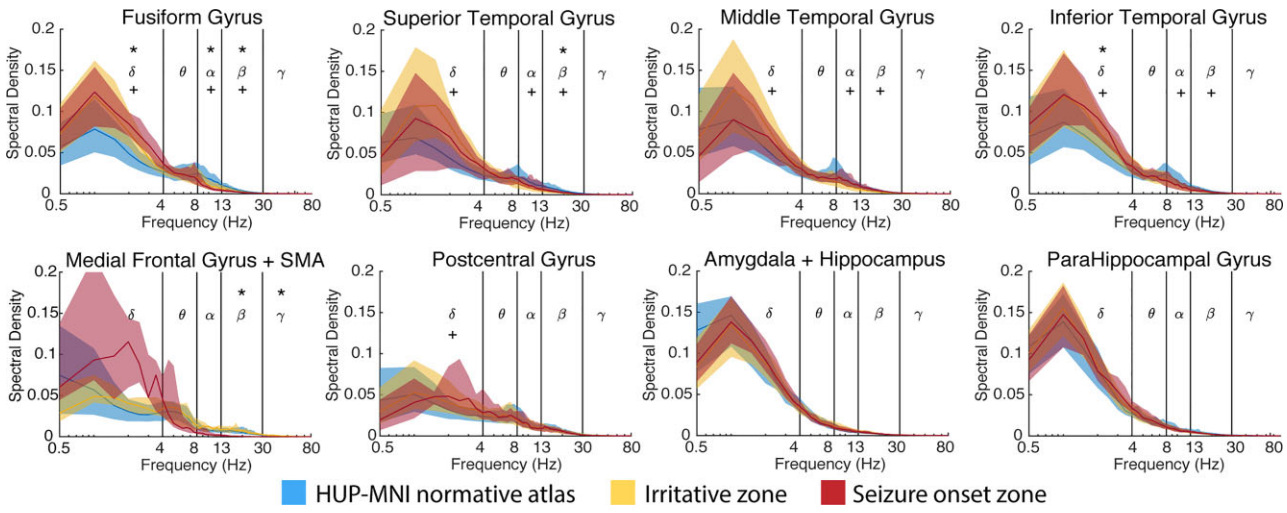

Figure 4 Univariate features are clinically useful. Within the eight most frequently resected regions in our dataset, spectral density is often different between the irritative zone, seizure onset zone, and the normative atlas. In each region and frequency band, we independently tested whether the median normalized band-power was different in the seizure onset zone versus the normative atlas, and the irritative zone versus the normative atlas. We completed this process for each of the following five frequency bands (delta: 0.5–4 Hz, theta: 4–8 Hz, alpha: 8–13 Hz, beta: 13–30 Hz, gamma: 30–80 Hz) and across all 20 regions. We thus Bonferroni corrected each test for 100 multiple comparisons. The asterisk above the Greek letters means the seizure onset zone is significantly different from normal, whereas the plus symbol below the letters means the irritative zone is significantly different from normal, Bonferroni corrected for 100 comparisons to $\alpha = 0.0005$. The shaded area represents the interquartile interval.

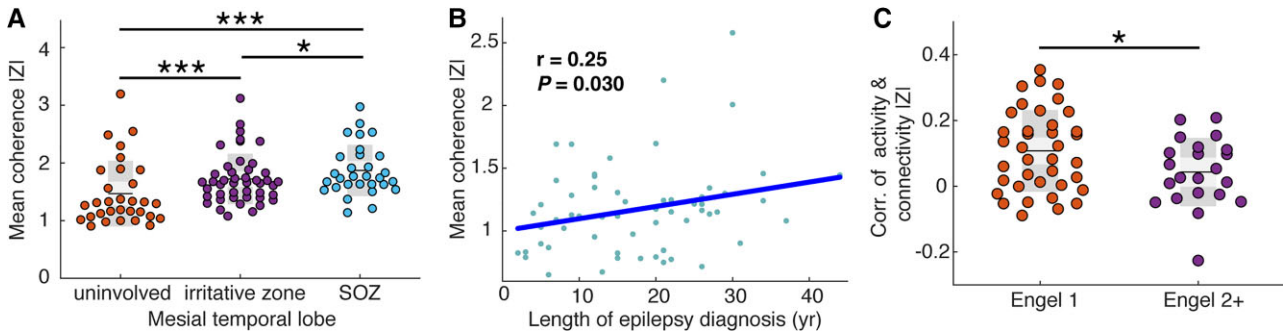

Figure 5 Bivariate features are clinically meaningful. (**A**) Mean coherence |z| is higher in the irritative zone (mean = 1.72 ± 0.43) and seizure onset zone (SOZ) (mean = 1.87 ± 0.44) compared with uninvolved brain (mean = 1.24 ± 0.39, rank-sum test one-tailed $P < 1 \times 10^{-5}$, Cohen's $d = 1.16$ and rank-sum test one-tailed $P < 1 \times 10^{-5}$, Cohen's $d = 1.51$ respectively). The seizure onset zone also has a higher |z| score versus the irritative zone (rank-sum test one-tailed $P = 0.045$, Cohen's $d = 0.34$) (**B**) Mean coherence absolute z-score is positively correlated with the length of epilepsy diagnosis (Pearson $r = 0.25$, $P = 0.030$). (**C**) The absolute z-score of power is more positively correlated with the absolute z-score of coherence within each good outcome patient compared with within each poor outcome patient (rank-sum test one-tailed $P = 0.037$, Cohen's $d = 0.56$).

we asked whether |z| scores of connectivity could do so (Fig. 5A), hypothesizing that the seizure onset zone would have the highest level of abnormality. For each mesial temporal lobe channel, we calculated the mean coherence |z| across the five frequency bands, and averaged these scores within mesial temporal lobe irritative, seizure onset and uninvolved zones for each patient. We observed a higher mean coherence |z| score across patients in both the irritative zone and seizure onset zone versus uninvolved channels (rank-sum test $P < 1 \times 10^{-5}$, Cohen's $d = 1.16$ and rank-sum test $P < 1 \times 10^{-5}$, Cohen's $d = 1.51$ respectively). We also observed a higher |z| score in the seizure onset zone versus the irritative zone (rank-sum test $P = 0.045$, Cohen's $d = 0.34$). These findings reveal that connectivity is an effective feature for distinguishing normal and abnormal brain, particularly in the mesial temporal lobe, which is a region of high clinical relevance in temporal lobe epilepsy.

We then sought to investigate whether connectivity abnormality could reveal broad aberrations in brain networks which were of clinical relevance (Fig. 5B). We hypothesized that patients who have had seizures for a longer period of time, measured in years from first seizure to iEEG implant, would have more abnormal brains. Indeed, we found a positive correlation between median connectivity abnormality and length of epilepsy diagnosis (Pearson $r = 0.25$, one-tailed $P = 0.030$). However, we did not observe a correlation between median activity abnormality and length of diagnosis (Pearson $r = -0.10$, one-tailed $P = 0.78$). This finding supports the notion that the cumulative burden of epilepsy progressively affects broadly distributed brain networks.

We additionally investigated the relationship between abnormalities in neural activity and functional connectivity (Fig. 5C). While we have established that both metrics are useful and provide complimentary information such as in the mesial temporal lobe, we expected that the correlations between these metrics would not be uniform across patients. In particular, we hypothesized that good outcome patients would have a higher concordance between abnormality in connectivity and neural activity compared with poor outcome subjects. We computed the Pearson correlation between spectral density and coherence |z| scores within each frequency band pair, and then calculated the average activity-connectivity correlation across the five bands. We found that good surgical outcome patients have a higher activity and connectivity abnormality correlation compared with poor surgical outcome patients (Pearson $r = 0.11 \pm 0.12$ versus $r = 0.04 \pm 0.10$, rank-sum test one-tailed $P = 0.037$, Cohen's $d = 0.56$). This finding emphasizes the complicated relationship between univariate and bivariate features and shows that poor outcome patients in particular may have discordant abnormality features.

Multivariate prediction of epileptogenicity

From the z-scores of each feature we sought to quantify the predicted epileptogenicity of each channel which could serve as an important tool in planning epilepsy surgery. To yield the best mapping of the epileptogenic zone, we trained a random forest classifier to classify nodes that were resected and part of the seizure onset zone from nodes which were deemed normal (Fig. 6A). We found that using both connectivity and activity |z|-scores yielded a superior classification cross-validation performance (AUC = 0.77) compared with either connectivity or spectral density features alone (AUC = 0.68 and 0.65, respectively). To ensure we did not bias our results by choosing absolute value of abnormality scores or the 75th percentile threshold of connectivity abnormality, we computed the AUC using alternative methods. We found that absolute abnormality scores better identified resected seizure onset zone nodes than directional scores and observed a trend towards better AUC with higher abnormality thresholds (Supplementary Fig. 7). We then asked which individual features were most important in making classifications of resected seizure onset zone versus normal tissue. We used the curvature test[35,36] to determine the change in out-of-bag predictor error when leaving out each feature and found that the most important features were delta band connectivity, delta band activity and gamma band connectivity (Fig. 6B).

We then sought to determine the predicted epileptogenicity of the irritative zone, given that the algorithm was only trained on the resected seizure onset zone nodes and normal nodes (Fig. 6C). We found that the irritative zone was predicted to have higher epileptogenicity compared with the uninvolved zone (rank-sum $P = 0.0093$), and also that the seizure onset zone had higher predicted epileptogenicity than the irritative zone (rank-sum $P = 0.012$). As expected from the cross-validation results, the seizure onset zone had higher predicted epileptogenicity than the uninvolved zone (rank-sum $P = 1.1 \times 10^{-4}$). These results suggest that the irritative zone is of intermediate abnormality compared with regions that can generate seizures and those that cannot. We also asked whether

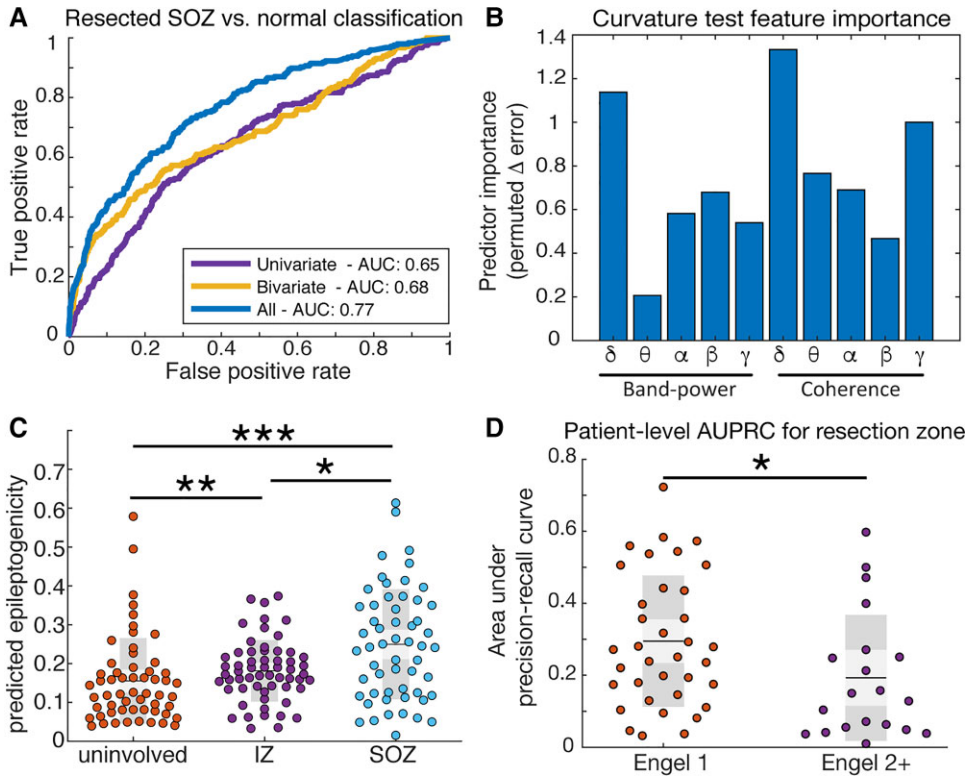

Figure 6 Multivariate identification of epileptogenic regions. (**A**) Classification for resected seizure onset zone (SOZ) versus normal brain. Using a combination of bivariate and univariate features yields a better AUC (0.77, blue curve) compared with only bivariate (0.68, yellow curve) or only univariate features (0.65, purple curve). (**B**) Curvature test of feature importance reveals delta band coherence is the single best feature, followed by delta band power and gamma band coherence. (**C**) The irritative zone (IZ) has an intermediate level of predicted epileptogenicity compared with the seizure onset zone (rank-sum $P = 0.012$, Cohen's $d = 0.59$) and uninvolved brain (rank-sum $P = 0.0093$, Cohen's $d = 0.27$). (**D**) Quantifying the patient-specific area under the precision recall curve for the seizure onset zone reveals a better performance for Engel 1 subjects versus Engel 2+ subjects (AUPRC 0.25 ± 0.17 versus 0.14 ± 0.11, rank-sum $P = 0.013$, Cohen's $d = 0.78$).

good and poor outcome patients had different patient-level performance of predicted epileptogenicity (Fig. 6D). We found that the precision-recall tradeoff for resected tissues was higher in good outcome versus poor outcome patients (AUPRC 0.25 ± 0.17 versus 0.14 ± 0.11, rank-sum $P = 0.013$, Cohen's $d = 0.78$), implying that the predicted nodes were more often resected in good outcome patients. Of the 60 subjects in the HUP cohort, 40 had higher mean epileptogenicity within the resection zone than outside of it, whereas our approach would have suggested an alternate approach in 20 subjects (Supplementary Fig. 8). However, we did not observe a difference in outcome groups.

We finally sought to illustrate how normative atlas mapping could be an effective strategy for guiding epilepsy surgery through three clinical cases. The first case (Fig. 7A) corresponds to a good outcome (Engel 1A) patient with parietal lobe epilepsy, in which high levels of predicted epileptogenicity cluster in and around the resection zone. The second case (Fig. 7B) corresponds to a good outcome (Engel 1B) patient with temporal lobe epilepsy in which high levels of predicted epileptogenicity cluster in and near the resection zone. The third case (Fig. 7C) corresponds to a poor outcome (Engel 2A) patient which underwent a right temporal lobe laser but did not become seizure free. The ablated nodes had moderate levels of abnormality. However, the contralateral mesial temporal lobe from which spikes were observed to originate had a higher level of predicted epileptogenicity, suggesting that this region might have been a better surgical target. Overall, these examples are mean to demonstrate that examining these spatial maps may help clinicians select between hypothesized epileptogenic zones during epilepsy surgical evaluation without the need for directly recording seizures on in hospital iEEG, which some investigators suggest may give inaccurate localization compared with seizures recorded out of hospital over longer periods of time[37,38].

Stability of interictal abnormalities over time

To test the stability of our normative atlas mapping approach, we first tested whether features of neural activity and functional connectivity remain stable at different levels of antiepileptic drug dosing. While many patients undergo antiepileptic drug withdrawal during iEEG implantation to provoke seizures, the pattern and extent of withdrawal is often heterogeneous. In three HUP patients we compared 60-s clips recorded on days of full antiepileptic drug dosing, with clips recorded 24 h away from the most recent dose after a taper. We found high correlations in the values of spectral density (mean Pearson $r = 0.72$) and coherence (mean Pearson $r = 0.75$) between these states (Supplementary Fig. 9). While we could not ensure the same antiepileptic drug loading across all patients, we further tested the stability of abnormality scores and epileptogenicity prediction in two additional 60-s clips selected >1 h away from our initial recordings. We observed high correlations in patient-specific abnormality $|z|$ scores across all 10 spectral density and coherence features (mean Pearson $r = 0.57$, Supplementary Fig. 10A) and

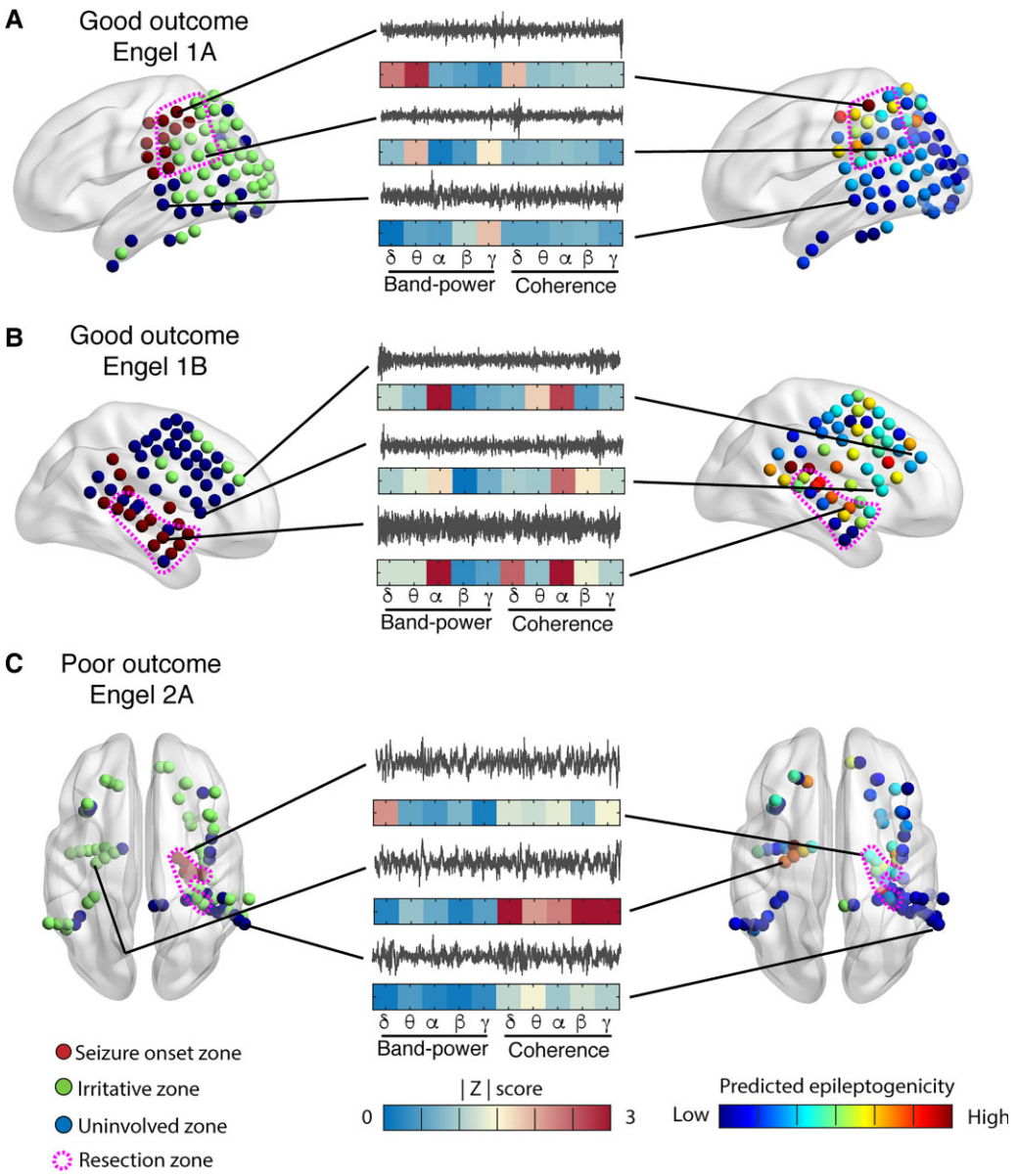

Figure 7 Mapping predicted epileptogenicity from abnormality scores. *Left*: Distribution of electrode contacts on surface of brain (red: seizure onset zone, green: irritative zone, blue: uninvolved zone, pink dotted outline: resection zone). *Middle*: Recordings from a channel in the seizure onset, irritative and uninvolved zones (grey) and their |*z*| scores (blue to red) for each of the 10 features. *Right*: Predicted epileptogenicity from the random forest model at each electrode location (blue to red). (**A**) Good outcome (Engel 1A) patient with parietal lobe epilepsy, in which high levels of predicted epileptogenicity cluster in and near the resection zone. (**B**) Good outcome (Engel 1B) patient with temporal lobe epilepsy in which high levels of predicted epileptogenicity cluster in and near the resection zone. (**C**) Poor outcome (Engel 2A) patient underwent a right temporal lobe laser ablation with minimal improvement. The ablated nodes had low levels of abnormality; however, the contralateral mesial temporal lobe from which spikes were observed to originate had a higher level of predicted epileptogenicity and could have been a better surgical target.

further observed a significant correlation between predicted epileptogenicity in 54 out of 60 patients (mean Pearson $r = 0.53$, Supplementary Fig. 10B). These findings concur with past work showing stability of epileptogenic zone identification from iEEG connectivity across time[14] and support the generalizability of our methods as uncovering a patient-specific fingerprint of interictal epileptogenicity.

Discussion

Developing new approaches to treating medicine-refractory seizures requires a better understanding of the relationship between the abnormal brain and epilepsy. Due to the brain's vast heterogeneity in structure and function, it seems unlikely that any single interictal biomarker will universally distinguish normal from abnormal tissue. We have demonstrated that normative iEEG mapping using only short clips of interictal data provides a flexible framework to identify epileptogenic regions and may explain several clinically important phenomena: namely, that the irritative zone is of intermediate abnormality between normal and seizure onset regions and that abnormalities in functional connectivity likely increase with longer diagnoses of epilepsy.

Our finding that mapping neural activity and functional connectivity together is superior to using either individually sheds light

on an important debate in epilepsy surgery: It is not clear whether epilepsy should be viewed as a focal problem within a network (and thus adequately probed by univariate methods which consider each channel independently) or as a broader, integrated network disorder (thus required concerted study of connectivity using multivariate methods)[6]. Our findings provide evidence for the utility and integration of both frameworks to best understand how epilepsy affects the brain. In particular, neocortex may manifest abnormalities due to epilepsy by changes in the spectral content of oscillatory activity, whereas epileptogenic tissue in the mesial temporal lobe may undergo changes in baseline connectivity. Our approach to normative iEEG mapping provides a flexible and generalizable framework for exploring each of these hypotheses at both the individual patient and group levels and may serve as a tool to target epilepsy surgery using the best metric for each anatomic region.

Our study adds to a growing body of work on normative analysis of intracranial EEG.[23,24,39,40] We directly built upon the work of Frauscher *et al*. 2018,[23] in which the authors demonstrated the approach of aggregating curated normative data and showed that spectral features including peak frequencies differ throughout cortical regions. Our extension demonstrates that the spectral parameters of interictal iEEG generalize across centres, and that deviations from normal frequency content are indeed indicative of regions that can manifest epileptic activity. We also adapted a multi-patient functional connectivity approach from Betzel *et al*., 2018,[24] in which the authors demonstrated that integrating adjacency matrices across patients provides group-level electrocortiograph connectivity that closely mirrors functional MRI connectivity, tracts white matter pathways, and is influenced by gene co-expression. Here, we have confirmed that deviations from expected, normative connectivity indeed can also distinguish potentially epileptogenic regions. Another recent study has demonstrated the value of normative modelling in mapping epileptogenic tissues using univariate spectral features.[40] Our study reproduces some of these results on a different dataset while also including the network connectivity measurements. We speculate that combining data from multiple centres can accelerate our efforts to develop important clinical tools that routinely use normative modelling to map epileptic networks.

Our finding that abnormalities in delta power, delta connectivity and gamma connectivity are the most important contributors in predicting epileptogenicity aligns with findings of previous studies. Focal slowing activity recorded in the delta frequency range is an electrographic marker of cerebral dysfunction[41] and correlates with medically intractable seizures. Analysing power and coherence abnormalities, Walker *et al*.[42] suggested that normalization of focal slowing by neurofeedback training can render patients seizure-free. Furthermore, slow-wave power can help localize the seizure onset zone[43] and is associated with focal structural lesions on MRI such as cortical malformations.[11] In contrast, many studies have reported HFOs as a promising marker of seizure onset zone and post-surgery outcomes. HFOs originate from functionally isolated areas and their presence correlates with gamma frequency band.[44,45] While the multicentre dataset in our study only contained frequency content from 0.5–80 Hz, higher frequency spectra such as the ripple (80–250 Hz) and fast ripple (250–500 Hz) bands contain additional pathologic HFO activity. Still, it is crucial to distinguish these pathological HFOs from normal physiological HFOs, such as those which occur during cognitive processes.[46–48] Recent work has used an analogous atlas approach[39] to differentiate pathological from physiological HFOs, and we envision that extending our normative iEEG atlas into higher frequency bands and integrating HFO content would allow us to better identify epileptogenic zones.

Normative atlas modelling also provides an important illustration of clinically relevant phenomena. Previously, others have reported that an increasing length of diagnosis is correlated with increased cross-hippocampal connectivity on functional MRI.[49] We validate and extend those findings by confirming their presence on intracranial EEG, showing that these abnormalities may be present in other regions, and that they are not explained by changes in electrographic activity. Indeed, our observations provide further evidence for epilepsy as a dynamic disorder, causing progressive changes in the brain over time. Importantly, we also find distributed abnormalities even in putatively uninvolved regions of the brain, even in patients that achieve good surgical outcome. These changes have been observed as well in similar studies of structural connectivity.[27] It is unclear whether these abnormalities are pathologic, as they could be compensatory for regions which have lost their normal function due to epileptic processes, such as mesial temporal sclerosis. Furthermore, even if they are pathologic, it is possible they may not become clinically meaningful on the timescale of our study and could contribute to late relapse many years after surgery.

Limitations and future directions

Our study represents a significant foray into applying full-brain atlas approaches to iEEG, with the goal of developing rigorous, quantitative methods that can be applied across centres to guide epilepsy surgery but comes with several limitations. One of these is that the assumption of normal activity and connectivity in uninvolved brain regions in individuals with medication -resistant epilepsy may not be universally valid. For example, uninvolved regions may exert inhibitory activity on a seizure focus as part of an inhibitory surround and could have abnormal activity as a result of this heightened inhibition. Indeed, even in good outcome patients, abnormalities in structural connectivity are observed outside of the resection zone[27] and may not be significant enough to cause seizures. Future work and data sharing across centres could address this by incorporating patients implanted with iEEG for purposes such as treating facial pain[50] or for underlying psychiatric conditions, in which no epileptic foci exist.

Another significant limitation is the spatial scale at which we map activity and connectivity. In this study we focus on connectivity between gross anatomic regions, while many of the aberrations in connectivity exist within regions of interest and thus could not be probed by our current approach. However, the natural step would be to break up automated anatomical labelling regions into even smaller parcellations, and such atlases of up to 600 regions have been used by our group in different contexts.[51] Even with 166 patients—which represents one of the largest published patient cohorts in a computational iEEG study—we did not have dense enough coverage in every region to have sufficient spatial granularity to evaluate more areas. However, as we show the power of building upon previously established datasets, we hope for others to further build upon our normative atlas mapping, which could allow this approach to be taken in the future. A much larger cohort could also allow us to calculate normative features across patients rather than across channels. This step could also ensure that all possible connections in the functional connectivity atlas are represented and have sufficient samples for the median and variance in connectivity to be accurately estimated.

The finding that one third of our subjects, including those who achieved seizure freedom, would have a different surgical approach suggested by our model is not altogether surprising. In some of these subjects, our predicted epileptogenic tissues may have also served as a feasible surgical strategy, whereas in others it is possible that truly epileptogenic tissues were unsampled by iEEG or did not have clear interictal abnormalities. Furthermore, eloquent cortex containing important motor and speech function must be avoided even when seizures originate from those regions. Additionally, it is possible that the spatial patterns of epileptogenicity are more important than their presence or degree. Further study is required to better understand which groups of patients could undergo epilepsy surgery guided purely from interictal findings versus those for which ictal recordings are critical.

To expand the utility of our atlas of iEEG connectivity for epilepsy surgery, the natural next step is to join our approach with similar methods in neuroimaging. Doing so may allow for investigators to identify abnormal connections in regions that are not typically implanted by iEEG, such as central grey matter structures including the thalamus, which is implicated in seizure generation and propagation. Furthermore, combining our approach with diffusion tensor imaging could help answer whether functional connectivity abnormalities as measured by iEEG are highly correlated to structural abnormalities, or whether these phenomena are only loosely related. Finally, future work could explore the utility of similar methods applied to non-invasive, high-density scalp EEG. Using full-brain iEEG atlas approaches could enable clinicians to better understand the relationship between structure and function and might ultimately allow iEEG to be replaced with fully non-invasive studies in some patients.

Conclusions

In this study we demonstrate the feasibility of using an atlas of iEEG for brain mapping in patients with drug-resistant epilepsy undergoing surgical evaluation. We show that clinically abnormal regions including the seizure onset zone and the irritative zone are detectable by the z-score of quantitative measures against the normative atlas. We also demonstrate that connectivity augments univariate measures of activity, particularly in the mesial temporal lobe, and show good classification of seizure onset zone versus normal channels. Through extensive data sharing we may soon reach adequate accuracy and brain coverage to use the atlas method as a preferred quantitative method for identifying the epileptogenic zone from intracranial EEG which could offer a substantial improvement for epilepsy surgery outcomes.

Acknowledgements

The authors would like to thank Jacqueline Boccanfuso for her help in data management. The citation diversity statement is available in the Supplementary material.

Funding

J.B. acknowledges funding from NIH 6T32NS091006. B.L. acknowledges funding from the Pennsylvania Tobacco Fund, NINDS R01: N.S. and R56099348, NIH DP1NS122038, the Mirowski Family Foundation, Jonathan Rothberg, and Neil and Barbara Smit. K.A.D acknowledges funding from NINDS R01NS116504, the Thornton Foundation and the Pennsylvania Tobacco Fund. N.S. acknowledges funding from NINDS R01NS116504, NIH DP1: NS122038.

Competing interests

The authors report no competing interests.

Supplementary material

Supplementary material is available at *Brain* online.

References

1. Kwan P, Schachter SC, Brodie MJ. Drug-resistant epilepsy. *N Engl J Med*. 2011;365:919–926.
2. Jehi L. The epileptogenic zone: concept and definition. *Epilepsy Curr*. 2018;18(1):12–16.
3. Téllez-Zenteno JF, Dhar R, Wiebe S. Long-term seizure outcomes following epilepsy surgery: a systematic review and meta-analysis. *Brain*. 2005;128(5):1188–1198.
4. Wiebe S, Blume WT, Girvin JP, Eliasziw M. A randomized, controlled trial of surgery for temporal-lobe epilepsy. *N Engl J Med*. 2001;345(5):311–318.
5. Parvizi J, Kastner S. Promises and limitations of human intracranial electroencephalography. *Nat Neurosci*. 2018;21:474–483.
6. Zaveri HP, Schelter B, Schevon CA, *et al*. Controversies on the network theory of epilepsy: debates held during the ICTALS 2019 conference. *Seizure*. 2020;78:78–85.
7. Vakharia VN, Duncan JS, Witt J-A, Elger CE, Staba R, Engel J. Getting the best outcomes from epilepsy surgery. *Ann Neurol*. 2018;83(4):676–690.
8. Lagarde S, Buzori S, Trebuchon A, *et al*. The repertoire of seizure onset patterns in human focal epilepsies: determinants and prognostic values. *Epilepsia*. 2019;60(1):85–95.
9. Conrad EC, Tomlinson SB, Wong JN, *et al*. Spatial distribution of interictal spikes fluctuates over time and localizes seizure onset. *Brain*. 2020;143(2):554–569.
10. Hufnagel A, Dumpelmann M, Zentner J, Schijns O, Elger CE. Clinical relevance of quantified iIntracranial interictal spike activity in presurgical evaluation of epilepsy. *Epilepsia*. 2000;41(4):467–478.
11. Noh BH, Berg AT, Nordli DR. Concordance of MRI lesions and EEG focal slowing in children with nonsyndromic epilepsy. *Epilepsia*. 2013;54(3):455–460.
12. Khambhati AN, Davis KA, Lucas TH, Litt B, Bassett DS. Virtual Cortical Resection Reveals Push-Pull Network Control Preceding Seizure Evolution. *Neuron*. 2016;91(5):1170–1182.
13. Shah P, Bernabei JM, Kini L, *et al*. High interictal connectivity within the resection zone is associated with favorable postsurgical outcomes in focal epilepsy patients. *NeuroImage Clin*. 2019;23:101908.
14. Wang Y, Sinha N, Schroeder GM, *et al*. Interictal intracranial electroencephalography for predicting surgical success: the importance of space and time. *Epilepsia*. 2020;61(7):1417–1426.
15. Sinha N, Dauwels J, Kaiser M, *et al*. Predicting neurosurgical outcomes in focal epilepsy patients using computational modelling. *Brain*. 2017;140(2):319–332.
16. Goodfellow M, Rummel C, Abela E, Richardson MP, Schindler K, Terry JR. Estimation of brain network ictogenicity predicts outcome from epilepsy surgery. *Sci Rep*. 2016;6(1):29215.
17. Li A, Chennuri B, Subramanian S, *et al*. Using network analysis to localize the epileptogenic zone from invasive EEG recordings in intractable focal epilepsy. *Netw Neurosci*. 2018;2(2):218–240.

18. Narasimhan S, Kundassery KB, Gupta K, *et al*. Seizure-onset regions demonstrate high inward directed connectivity during resting-state: an SEEG study in focal epilepsy. *Epilepsia*. 2020; 61(11):2534–2544.
19. Burns SP, Santaniello S, Yaffe RB, *et al*. Network dynamics of the brain and influence of the epileptic seizure onset zone. *Proc Natl Acad Sci USA*. 2014;111(49):E5321–E5330.
20. Kini LG, Bernabei JM, Mikhail F, *et al*. Virtual resection predicts surgical outcome for drug-resistant epilepsy. *Brain*. 2019;142(12): 3892–3905.
21. Conrad EC, Bernabei JM, Kini LG, *et al*. The sensitivity of network statistics to incomplete electrode sampling on intracranial EEG. *Netw Neurosci*. 2020;4(2):484–506.
22. Bernabei JM, Arnold TC, Shah P, *et al*. Electrocorticography and stereo EEG provide distinct measures of brain connectivity: implications for network models. *Brain Commun*. 2021;3:fcab156.
23. Frauscher B, von Ellenrieder N, Zelmann R, *et al*. Atlas of the normal intracranial electroencephalogram: neurophysiological awake activity in different cortical areas. *Brain*. 2018;141(4): 1130–1144.
24. Betzel RF, Medaglia JD, Kahn AE, Soffer J, Schonhaut DR, Bassett DS. Structural, geometric and genetic factors predict interregional brain connectivity patterns probed by electrocorticography. *Nat Biomed Eng*. 2019;3:902–916.
25. Balatskaya A, Roehri N, Lagarde S, *et al*. The "Connectivity Epileptogenicity Index" (cEI), a method for mapping the different seizure onset patterns in StereoElectroEncephalography recorded seizures. *Clin Neurophysiol*. 2020;131(8):1947–1955.
26. Hatton S, Huynh K, Bonilha L, *et al*. White matter abnormalities across different epilepsy syndromes in adults: an ENIGMA-Epilepsy study. *Brain*. 2020;143(8):2454–2473.
27. Sinha N, Wang Y, da Silva NM, *et al*. Structural brain network abnormalities and the probability of seizure recurrence after epilepsy surgery. *Neurology*. 2021;96(5):e758–e771.
28. Sinha N, Peternell N, Schroeder GM, *et al*. Focal to bilateral tonic–clonic seizures are associated with widespread network abnormality in temporal lobe epilepsy. *Epilepsia*. 2021;62(3):729–741.
29. Parkes L, Moore TM, Calkins ME, *et al*. Transdiagnostic dimensions of psychopathology explain individuals' unique deviations from normative neurodevelopment in brain structure. *Transl Psychiatry*. 2021;11(1):232.
30. Avants B, Tustison N, Song G. Advanced Normalization Tools (ANTS). *Insight J*. 2009;2(365):1–35.
31. Yushkevich PA, Piven J, Hazlett HC, *et al*. User-guided 3D active contour segmentation of anatomical structures: significantly improved efficiency and reliability. *Neuroimage*. 2006;31(3): 1116–1128.
32. Welch PD. The use of fast fourier transform for the estimation of power spectra: a method based on time averaging over short, modified periodograms. *IEEE Trans Audio Electroacoust*. 1967; 15(2):70–73.
33. Davis J, Goadrich M. The Relationship Between Precision-Recall and ROC Curves. In: Proceedings of the 23rd International Conference on Machine Learning; 2006.
34. Kini LG, Davis KA, Wagenaar JB. Data integration: combined Imaging and Electrophysiology data in the cloud. *Neuroimage*. 2016;124:1175–1181.
35. Loh W-Y. Regression trees with unbiased variable selection and interaction detection. *Stat Sin*. 2002;12:361–386.
36. Loh W-Y, Shih Y-S. Split selection methods for classification trees. *Stat Sin*. 1997;7:815–840.
37. DiLorenzo DJ, Mangubat E, Rossi M, Byrne R. Chronic unlimited recording electrocorticography-guided resective epilepsy surgery: technology-enabled enhanced fidelity in seizure focus localization with improved surgical efficacy. *J Neurosurg*. 2014; 120(6):1402–1414.
38. King-Stephens D, Mirro E, Weber PB, *et al*. Lateralization of mesial temporal lobe epilepsy with chronic ambulatory electrocorticography. *Epilepsia*. 2015;56(6):959–967.
39. Kuroda N, Sonoda M, Miyakoshi M, *et al*. Objective interictal electrophysiology biomarkers optimize prediction of epilepsy surgery outcome. *Brain Commun*. 2021;3(2):fcab042.
40. Taylor PN, Papasavvas CA, Owen TW, *et al*. Normative brain mapping of interictal intracranial EEG to localize epileptogenic tissue. *Brain*, 2022;145(3):939–949.
41. Lundstrom BN, Boly M, Duckrow R, Zaveri HP, Blumenfeld H. Slowing less than 1 Hz is decreased near the seizure onset zone. *Sci Rep*. 2019;9(1):1–10.
42. Walker JE. Power spectral frequency and coherence abnormalities in patients with intractable epilepsy and their usefulness in long-term remediation of seizures using neurofeedback. *Clin EEG Neurosci*. 2008;39(4):203–205.
43. Lundstrom BN, Meisel C, Van Gompel J, Stead M, Worrell G. Comparing spiking and slow wave activity from invasive electroencephalography in patients with and without seizures. *Clin Neurophysiol*. 2018;129(5):909–919.
44. Zweiphenning WJEM, Keijzer HM, van Diessen E, *et al*. Increased gamma and decreased fast ripple connections of epileptic tissue: a high-frequency directed network approach. *Epilepsia*. 2019;60(9):1908–1920.
45. Zweiphenning WJEM, Van 't Klooster MA, Van Diessen E, *et al*. High frequency oscillations and high frequency functional network characteristics in the intraoperative electrocorticogram in epilepsy. *Neuroimage Clin*. 2016;12:928–939.
46. Blanco JA, Stead M, Krieger A, *et al*. Data mining neocortical high-frequency oscillations in epilepsy and controls. *Brain*. 2011;134(10):2948–2959.
47. Matsumoto A, Brinkmann BH, Stead SM, *et al*. Pathological and physiological high-frequency oscillations in focal human epilepsy. *J Neurophysiol*. 2013;110(8):1958.
48. Kucewicz MT, Cimbalnik J, Matsumoto JY, *et al*. High frequency oscillations are associated with cognitive processing in human recognition memory. *Brain*. 2014;137(8):2231–2244.
49. Morgan VL, Rogers BP, Sonmezturk HH, Gore JC, Abou-Khalil B. Cross hippocampal influence in mesial temporal lobe epilepsy measured with high temporal resolution functional magnetic resonance imaging. *Epilepsia*. 2011;52(9):1741–1749.
50. Warren CP, Hu S, Stead M, Brinkmann BH, Bower MR, Worrell GA. Synchrony in normal and focal epileptic brain: the seizure onset zone is functionally disconnected. *J Neurophysiol*. 2010; 104(6):3530–3539.
51. Shah P, Ashourvan A, Mikhail F, *et al*. Characterizing the role of the structural connectome in seizure dynamics. *Brain*. 2019; 142(7):1955–1972.